Biochimica et Biophysica Acta 1862 (2016) 82–92

Contents lists available at ScienceDirect

Biochimica et Biophysica Acta

journal homepage: www.elsevier.com/locate/bbadis

S-adenosylhomocysteine induces inflammation through NFkB: A possible role for EZH2 in endothelial cell activation

Madalena Barroso [a,b], Derrick Kao [a], Henk J. Blom [c], Isabel Tavares de Almeida [b], Rita Castro [b,d], Joseph Loscalzo [a], Diane E. Handy [a,*]

[a] Cardiovascular Division, Department of Medicine, Brigham and Women's Hospital and Harvard Medical School, Boston, MA, USA
[b] Research Institute for Medicines (iMed.ULisboa), Faculty of Pharmacy, University of Lisbon, Lisbon, Portugal
[c] Laboratory of Clinical Biochemistry and Metabolism, Department of General Pediatrics, Adolescent Medicine and Neonatology, University Medical Centre Freiburg, Freiburg, Germany
[d] Department of Biochemistry and Human Biology, Faculty of Pharmacy, University of Lisbon, Lisbon, Portugal

ARTICLE INFO

Article history:
Received 8 July 2015
Received in revised form 29 September 2015
Accepted 22 October 2015
Available online 24 October 2015

Keywords:
S-adenosylhomocysteine
Endothelial activation
Adhesion molecules
NFkB
Methylation
EZH2

ABSTRACT

S-adenosylhomocysteine (SAH) can induce endothelial dysfunction and activation, contributing to atherogenesis; however, its role in the activation of the inflammatory mediator NFkB has not been explored. Our aim was to determine the role of NFkB in SAH-induced activation of endothelial cells. Furthermore, we examined whether SAH, as a potent inhibitor of S-adenosylmethionine-dependent methyltransferases, suppresses the function of EZH2 methyltransferase to contribute to SAH-induced endothelial cell activation. We found that excess SAH increases the expression of adhesion molecules and cytokines in human coronary artery endothelial cells. Importantly, this up-regulation was suppressed in cells expressing a dominant negative form of the NFkB inhibitor, IkB. Moreover, SAH accumulation triggers the activation of both the canonical and non-canonical NFkB pathways, decreases EZH2, and reduces histone 3 lysine 27 trimethylation. EZH2 knockdown recapitulated the effects of excess SAH on endothelial activation, i.e., it induced NFkB activation and the subsequent up-regulation of adhesion molecules and cytokines. Our findings suggest that suppression of the epigenetic regulator EZH2 by excess SAH may contribute to NFkB activation and the consequent vascular inflammatory response. These studies unveil new targets of SAH regulation, demonstrating that EZH2 suppression and NFkB activation mediated by SAH accumulation may contribute to its adverse effects in the vasculature.

1. Introduction

S-adenosylhomocysteine (SAH) is an inhibitor of cell methyltransferases that accumulates during hyperhomocysteinemia. SAH-induced hypomethylation of DNA, protein, and RNA has been associated with vascular disease [1–4]. Elevated homocysteine in plasma is an independent risk factor for cardiovascular diseases [5]. We and others have suggested that SAH is a key mediator of homocysteine-associated atherogenesis [1,6,7]. Our previous studies show that SAH can induce endothelial cell dysfunction and activation by decreasing nitric oxide production and increasing oxidative stress and leukocyte adhesion [1,8]. The molecular mechanisms by which SAH induces a pro-inflammatory phenotype are, however, not completely understood. Several studies have reported a role for the nuclear transcription factor kB (NFkB) in endothelial dysfunction and atherosclerosis [9–11].

NFkB is a major regulator of important cell processes, such as inflammation, immunity, cellular proliferation, and apoptosis [12,13]. NFkB complexes are composed of homo- or heterodimers of various NFkB family members, including p50, p52, p65 (RelA), RelB, and c-Rel [12,14]. The NFkB pathway can be triggered by several stimuli, including inflammatory cytokines such as tumor necrosis factor-α (TNF-α) and interleukin-1β (IL-1β), which initiate the classical pathway; or other stimuli such as the CD40 ligand and lymphotoxin β, which trigger the alternative NFkB pathway [12,13].

DNA and histones are well studied targets of methyltransferases that can modulate important cellular processes. Enhancer of zeste homolog 2 (EZH2) is the catalytic core of the polycomb repressive complex (PRC) 2 and establishes the major mark of transcriptional repression in mammalian cells: the trimethylation of lysine 27 on histone 3 (H3K27me3) [15]. As an S-adenosylmethionine-dependent methyltransferase, EZH2 is a target for SAH-mediated inhibition. EZH2 modulates many cellular processes, including inflammation and cell adhesion, by targeting genes such as *IL1B* and *CDH13* [16]. The H3K27me3 mark can be removed by the Jumonji domain containing 3 (JMJD3) or the ubiquitously transcribed tetratricopeptide repeat on X chromosome (UTX) demethylases [17–19].

We previously used human umbilical vein endothelial cells (HUVEC) to investigate the role of excess SAH in endothelial activation. Our

* Corresponding author at: Brigham and Women's Hospital, 77 Avenue Louis Pasteur, NRB 0630L, Boston, MA 02115, USA.
E-mail address: dhandy@rics.bwh.harvard.edu (D.E. Handy).

http://dx.doi.org/10.1016/j.bbadis.2015.10.019
0925-4439/

findings showed that SAH-induced oxidative stress promotes an up-regulation of adhesion molecules [1]; however, the molecular mechanisms by which redox changes activate inflammatory responses under excess SAH were not completely resolved. Here, we analyze the effects of SAH on human coronary artery endothelial cells (HCAEC), and demonstrate the role of SAH-mediated hypomethylation on NFkB activation and modulation of pro-inflammatory signals. Additionally, we show that excess SAH suppresses the expression of EZH2 and that EZH2 knockdown mimics the endothelial cell responses to excess SAH, suggesting that the suppression of this methyltransferase may contribute to SAH-mediated endothelial dysfunction.

2. Materials and methods

2.1. Cell culture and treatments

Human coronary artery endothelial cells (HCAECs) were cultured at 37 °C in 5% CO_2. Cells were grown in EBM-2 supplemented (EGM-2-MV) medium (Lonza) without antibiotics. Experiments were performed between passages five and eight and with cells 70 to 80% confluent. Treatments with adenosine-2′,3′-dialdehyde (ADA) (Sigma) were performed for 48 h at 20 μM. Tumor necrosis factor-α (TNF-α) treatments (10 ng/mL; R&D systems) were performed for 24 h.

2.2. SAH and SAM analysis

SAH and SAM were measured in deproteinized cell extracts by tandem mass spectrometry as previously described [20].

2.3. Real-time PCR

RNeasy Mini kit (Qiagen) was used for RNA extraction. DNase (Qiagen) treatment was performed during the RNA extraction protocol, according to the manufacturer's instructions. After reverse-transcription using the Advantage RT-for-PCR kit (Clontech), cDNA was used for real-time PCR reactions with TaqMan Universal PCR Master Mix (Life Technologies) and specific gene expression primers (Life Technologies): *ACTB* (β-actin) (4352935E); *ICAM1* (Hs00164932_m1); *SELE* (Hs00950401_m1); *VCAM1* (Hs00365485_m1); *PECAM1* (Hs00169777_m1); *RELA* (Hs00153294_m1); *NFKB1* (Hs00231653_m1); *NFKB2* (Hs00174517_m1); *IL1B* (Hs01555410_m1); *TNFA* (Hs01113624_g1); *EZH2* (Hs00544833_m1); *KDM6B* (Hs00996325_g1); *CDKN1A* (Hs00355782_m1); *CDKN2A* (Hs00923894_m1). PCR reactions were performed using a PRISM 7900 HT Sequence Detector (Applied Biosystems). The ΔΔCT method was used for relative quantification using β-actin as the endogenous control.

2.4. Western blotting

Proteins were separated by SDS-PAGE before semi-dry transfer. After blocking, the following specific primary antibodies were used: anti-β-actin (Sigma-Aldrich), anti-ICAM-1 (Santa Cruz), anti-H3K27me3 (Epigentek), anti-VCAM-1, anti-IκBα, anti-p65, anti-NFKB2 p100/p52, anti-IL-1β, anti-EZH2, anti-CDKN1A, and anti-H3 (Cell Signaling). Secondary anti-rabbit HRP-linked antibody (Cell Signaling) was used for ECL-mediated (GE Healthcare Life Sciences) detection.

2.5. Nuclear protein extraction

Nuclear protein extracts were obtained with the NE-PER nuclear and cytoplasmic extraction reagents (Thermo Scientific) following the kit protocol.

2.6. NFKB inhibition

The dominant negative IkBα adenovirus (AdIkBDN) (Vector Biolabs) was used to overexpress a recombinant form of the IkBα, which is resistant to its phosphorylation-induced degradation. HCAEC infection with AdIkBDN was performed simultaneously with ADA treatment. An empty adenoviral vector was used as a control (AdCtrl) (Vector Biolabs).

2.7. Luciferase and β-galactosidase assays

A luciferase adenoviral expression vector (AdNFkB-Luc) (Vector Biolabs) controlled by a promoter containing five repeats of the NFkB enhancer element (TGGGGACTTTCCGC) was used to infect HCAECs that were simultaneously infected with a β-galactosidase expression vector (Vector Biolabs). HCAEC were infected with adenovirus for 24 h prior to treatments. Cell lysates were obtained using the reporter lysis buffer (Promega) and promptly used for the luciferase and β-galactosidase enzyme assays (Promega). Firefly luciferase activity was measured using the $20/20^n$ luminometer (Turner Biosystems), while β-galactosidase activity was measured by absorbance detection at 420 nm (SPECTRA MAX 190, Molecular Devices).

2.8. Histone extraction

Histone extracts were prepared using EpiQuik total histone extraction kit (Epigentek) following the manufacturer's instructions.

2.9. siRNA transfections

Transfections with small interference RNA (siRNA) were performed in OPTI-MEM medium (Life Technologies) using lipofectamine 2000 (Life Technologies) and a stealth siRNA to EZH2 (5′-GACCACAGUGUU ACCAGCAUUUGGA-3′) or a scrambled control siRNA (5′-GGUAGCGC CAAUCCUUACGUCUCUU-3′). The final siRNA concentration used was 52 nM.

2.10. Statistics

All of the experiments were repeated three to five times. Results are shown as mean ± standard deviation. Statistical significance of the differences between means was determined by Student's *t* test or ANOVA followed by post-hoc multiple comparisons using the Newman–Keuls test for experiments with two or more conditions, respectively.

3. Results

3.1. Endothelial cell activation by excess SAH

We previously showed that ADA-induced SAH hydrolase inhibition reduces the S-adenosylmethionine (SAM)/SAH ratio over 6-fold in HUVEC due to a significant accumulation in SAH. In HUVEC, this treatment results in increased expression of adhesion molecules [1]. In Fig. 1, we examined whether ADA modulates the expression of the adhesion molecules, intercellular adhesion molecule-1 (ICAM-1), vascular cell adhesion molecule-1 (VCAM-1), E-selectin, and platelet/endothelial adhesion molecule-1 (PECAM-1), in human endothelial cells derived from coronary artery (HCAECs), a type of endothelial cells more relevant to atherosclerotic vascular disease than HUVECs. In HCAEC, 48 h exposure to the ADA significantly increased SAH from 76 ± 19 to 1545 ± 478 pmol/mg ($p < 0.007$). Under SAH hydrolase inhibition, SAM was also modestly increased from 429 ± 23 to 514 ± 49 pmol/mg ($p < 0.05$) and the SAM/SAH ratio was significantly decreased from 5.81 ± 1.6 to 0.35 ± 0.09 ($p < 0.005$). After 48 h of incubation with the SAH hydrolase inhibitor, HCAECs showed a 4.0 ± 1.1- and

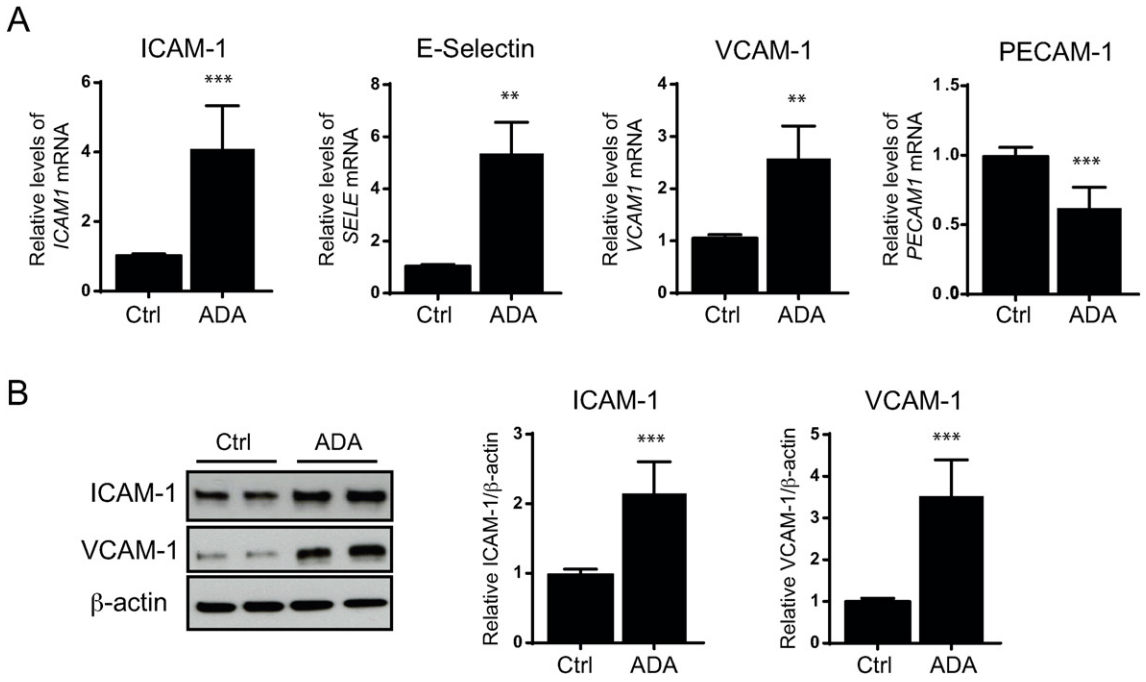

Fig. 1. SAH accumulation and cell activation. A, ICAM-1, E-selectin (encoded by the *SELE* gene), VCAM-1, and PECAM-1 transcript levels were measured by quantitative RT-PCR to determine the effects of ADA 20 μM (ADA) compared to control (Ctrl) (n = 3–5). B, Western blot analysis of ICAM-1 and VCAM-1 following ADA treatment for 48 h. Summary densitometry measurements for five independent experiments are shown on the right of the representative immunoblots. **p < 0.005, ***p < 0.0005 versus control.

2.5 ± 0.5-fold increase in ICAM-1 and VCAM-1 mRNA levels ($p < 0.005$), respectively (Fig. 1A), similar to our previous findings in HUVECs [1]. E-selectin transcripts were also increased by 5.2 ± 1.0-fold ($p < 0.005$), whereas ADA significantly decreased PECAM-1 transcript levels by 37.4 ± 13.4% ($p < 0.0005$) (Fig. 1A). Accordingly, ICAM-1 and VCAM-1 protein levels were up-regulated by 2.2 ± 0.4- and 3.5 ± 0.8-fold ($p < 0.0005$), respectively, in ADA-treated HCAECs (Fig. 1B).

3.2. NFkB pathway activation by excess SAH

We next examined whether ADA treatment activates the NFkB pathway. To do so, we initially monitored p50 and p65, as they are the most abundant NFkB components in the canonical pathway [21]. ADA treatment had no significant effect on the expression of the p50 and p65 encoding genes, *NFKB1* and *RELA*, respectively (Fig. 2A). Activation of the canonical pathway is usually marked by the phosphorylation and degradation of the NFkB inhibitory protein IkBα, releasing NFkB and allowing its migration to the nucleus [14]. In order to study this process, we assessed IkBα degradation and p65 translocation. After ADA treatment, IkBα levels decreased by 72.2 ± 17.1% ($p < 0.005$), and a 42.1 ± 17.5% increase of nuclear p65 protein was observed ($p < 0.05$; Fig. 2B & C). Taken together, these data support the notion that ADA induces activation of the NFkB canonical pathway. To confirm the effects of excess SAH on NFkB-induced transcriptional activation, we used an NFkB luciferase reporter construct (Fig. 2D). TNF-α was used as a positive control, as it is a well-known activator of NFkB in endothelial cells [22]. As expected, non-infected cells had no detectable luciferase activity, whereas infected cells treated with TNF-α for 24 h had a 4.4 ± 0.6-fold increase in luciferase activity compared with infected cells not exposed to TNF-α or ADA. Similarly, intracellular SAH accumulation significantly increased NFkB-dependent luciferase activity by 2.8 ± 0.3-fold ($p < 0.0005$).

IkBα degradation is induced after its phosphorylation at serine residues S32 and S36 [23]. To block NFkB activation, we overexpressed the dominant-negative mutant NF-kB inhibitor (IkBDN), which lacks S32 and S36 and cannot be targeted for degradation (Fig. 2E & F) [24]. Wild type IkBα levels (lower molecular weight) are reduced after ADA treatment whereas the recombinant IkBDN (higher molecular weight) is modestly up-regulated by ADA treatment (Fig. 2F). As shown in Fig. 2E & F, baseline adenoviral infection had no effect on the expression of adhesion molecules when compared to non-infected cells (NV). Upon ADA exposure, cells infected with the control adenovirus (AdCtrl) had a 4.2 ± 0.3-fold up-regulation of ICAM-1 mRNA levels ($p < 0.0005$). This effect was inhibited by the presence of the IkBDN ($p < 0.0005$). Similarly, VCAM-1 and E-selectin transcript levels were reduced by IkBDN to 13.7 ± 2.2% and 6.1 ± 1.5% ($p < 0.0005$), respectively, in ADA-treated cells. ADA significantly augmented ICAM-1 (1.6 ± 0.2-fold) and VCAM-1 (1.9 ± 0.3-fold) protein expression in cells transduced with the AdCtrl ($p < 0.05$). These effects were attenuated by expression of the IkBDN ($p < 0.0005$, Fig. 2F).

3.3. Alternative NFkB pathway activation

Unlike the canonical pathway, the non-canonical or alternative NFkB pathway is independent of IkBα and involves p100 phosphorylation and processing to the NFkB active subunit p52 [25]. We analyzed the activation of the non-canonical NFkB pathway by monitoring changes in the expression of *NFKB2* and its gene products, p100 and p52 (Fig. 3). There was a significant increase in *NFKB2* gene expression (1.8 ± 0.2-fold) following ADA treatment ($p < 0.0005$). Western blot analysis revealed a 1.8 ± 0.2-fold concomitant increase in p100 levels ($p < 0.05$) upon ADA exposure with evidence for increased p100 processing, as illustrated by the higher levels of p52 detectable under excess SAH compared to the control (2.5 ± 0.4-fold increase; $p < 0.005$).

We next used the adenoviral vector IkBDN to determine whether the NFkB canonical pathway modulates the non-canonical pathway (Fig. 3C & D). The presence of the control virus augmented the ADA-induced up-regulation of *NFKB2* gene expression compared to ADA-treated cells with no virus, increasing further ADA-induced NFkB2

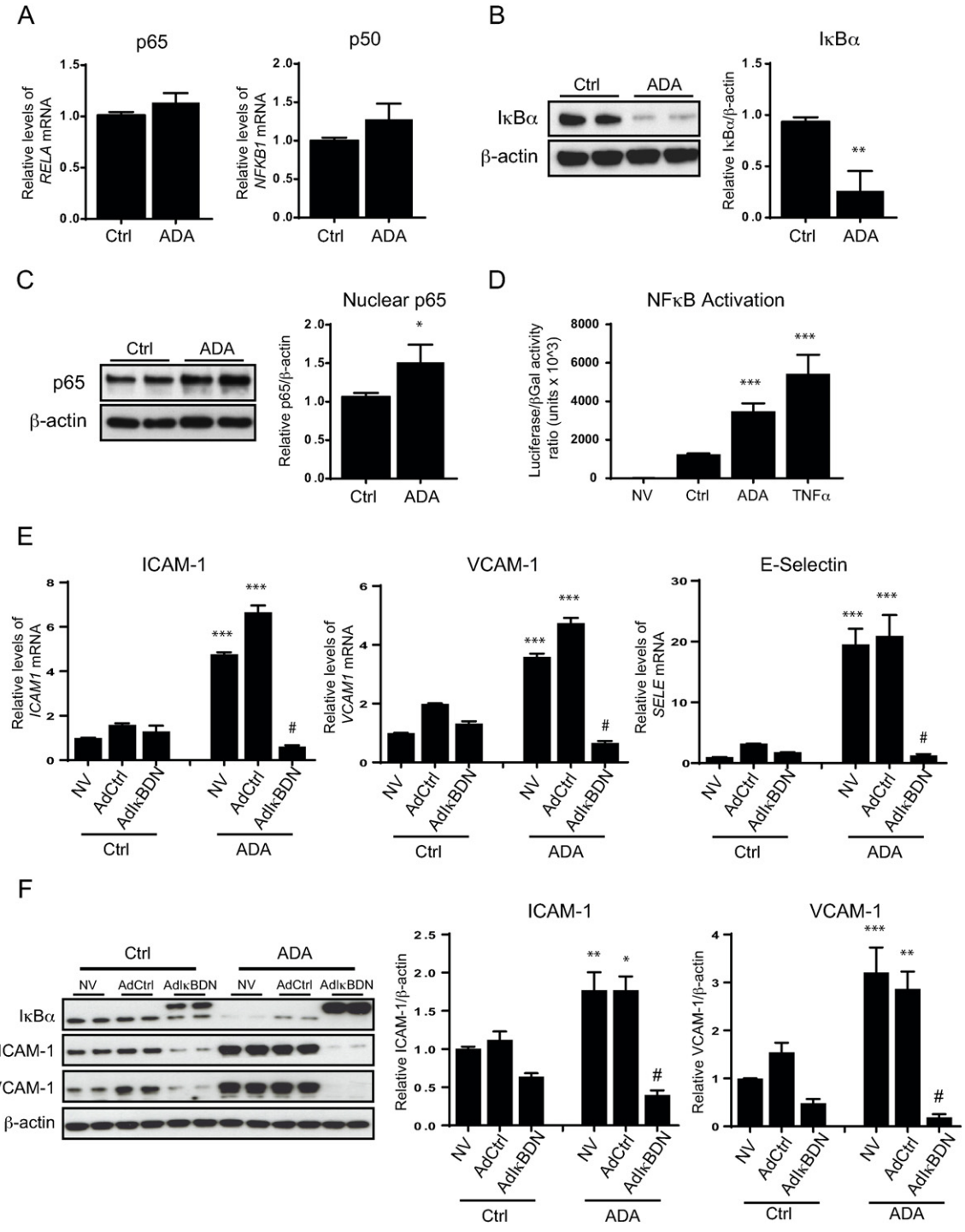

Fig. 2. NFkB pathway activation and its role in SAH-mediated up-regulation of adhesion molecules. A, ADA-mediated changes in *RELA* (p65) and *NFKB1* (p50) gene expression were measured by quantitative RT-PCR using β-actin as an endogenous control (n = 3). B, IkBα protein degradation induced by ADA was evaluated by Western blot. A representative blot is shown on the left and summary densitometry measurements on the right (n = 3). C, Nuclear levels of p65. Western blot was used to analyze nuclear extracts. Shown are a representative Western blot (left) and a graph of the average densitometry measurements (right, n = 3). D, The ability of ADA to promote NFkB-mediated transcription was analyzed using an NFkB luciferase reporter adenovirus construct simultaneously with a β-galactosidase vector (n = 4). Luciferase expression was normalized to β-galactosidase activity. Results are shown for uninfected HCAECs (NV) and infected cells without treatment (Ctrl) or treated with ADA for 48 h (ADA) or TNFα for 24 h (TNFα). E & F, Cells overexpressing dominant negative IkBα (AdIkBDN), infected with an empty control adenovirus (AdCtrl), and uninfected control cells (NV) were incubated in the presence or absence of ADA. E, Quantitative RT-PCR was used to study differences in mRNA levels of ICAM-1, VCAM-1, and E-selectin. F, Protein extracts were used for Western blot analysis. A representative immunoblot (left) and summary densitometry measurements (right) are shown (n = 3). Note that the recombinant IkBDN migrates more slowly than the endogenous IkBα. A, B and C. *$p < 0.05$, **$p < 0.005$, versus control. ANOVA, followed by the Newman–Keuls test for multiple comparisons, was used in the analysis shown in panels D, E and F. *$p < 0.05$, **$p < 0.005$, ***$p < 0.0005$, versus the corresponding condition without ADA treatment. #$p < 0.0005$, versus ADA treated cells with no virus or those infected with the AdCrl (ADA-AdCtrl).

mRNA levels 2.0 ± 0.04-fold ($p < 0.0005$) in the AdCtrl cells compared to ADA-treated cells with no virus. In contrast, ADA-induced expression of *NFKB2* was significantly attenuated by IkBDN ($p < 0.0005$). Accordingly, endothelial cells infected with the AdCtrl also manifested an increase in p52 (2.9 ± 0.6-fold; $p < 0.0005$) with ADA treatment, which was abolished by the presence of IkBDN ($p < 0.0005$, Fig. 3D).

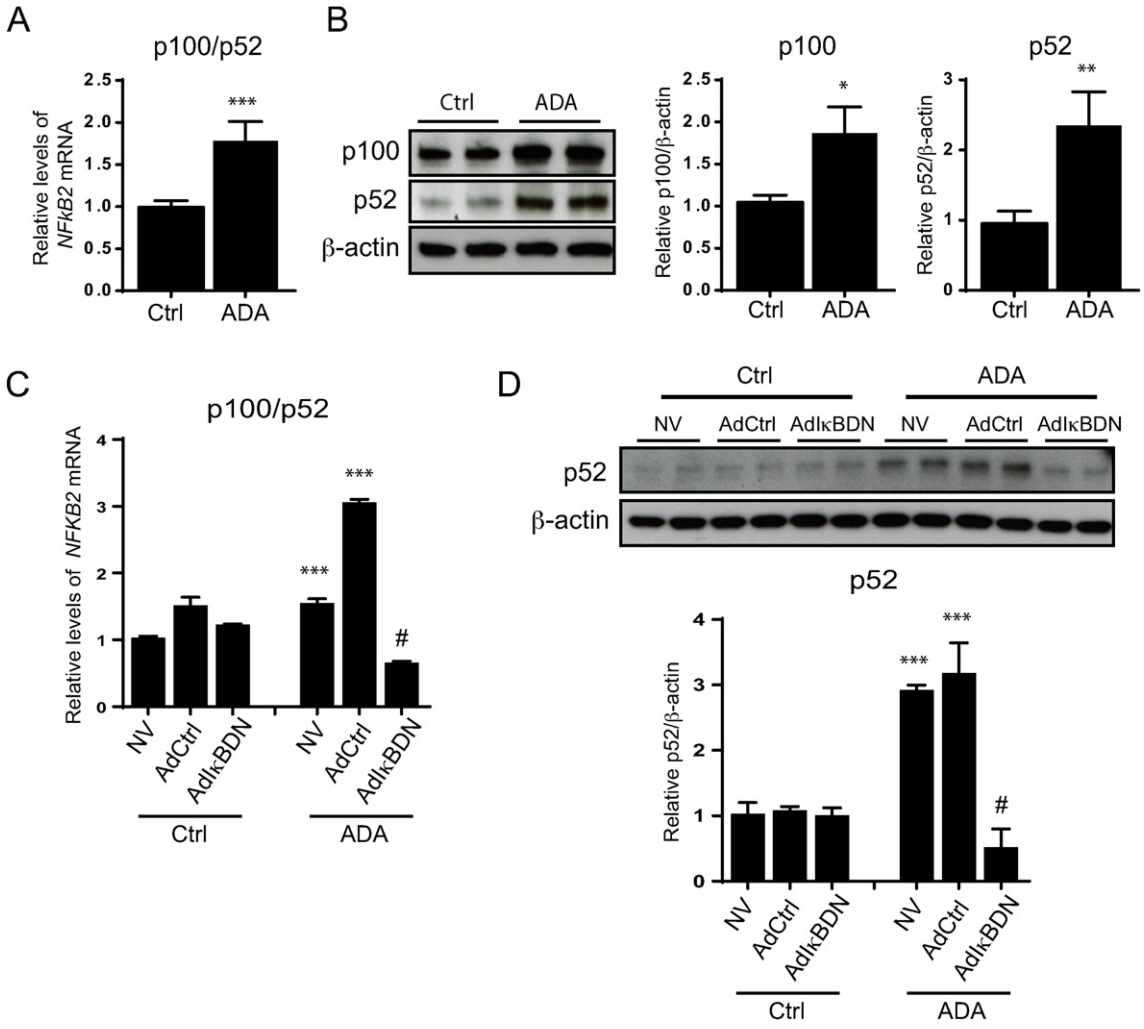

Fig. 3. Activation of the NFkB alternative pathway. A, *NFKB2* (p100/p52) transcript levels from control and ADA-treated cells were measured by quantitative RT-PCR (n = 4). *p < 0.05, **p < 0.005, ***p < 0.0005, versus control. B, Protein expression of p100 and p52 in HCAECs control and with ADA treatment. Representative Western blots (left) and summary densitometry analysis (right) are shown (n = 3). The statistical analysis was performed as in A. C, *NFKB2* mRNA levels under SAH accumulation, analyzed by quantitative RT-PCR, for cells infected with AdIkBDN, the control adenovirus (AdCtrl), or control uninfected cells (NV) (n = 3). ANOVA with multiple comparisons was used for statistical significance analysis. ***p < 0.0005 versus the correspondent no ADA condition. #p < 0.0005 versus ADA treated cells with no virus or infected with the AdCtrl. D, Western blot analysis of p52 expression in cells infected with AdIkBDN, AdCtrl, or NV that were treated or untreated with ADA. Representative blot is shown (top) with the densitometry measurements (below, n = 3). Statistical analysis was performed as in C.

3.4. SAH accumulation results in increased expression of pro-inflammatory cytokines

Interestingly, inflammatory cytokines, such as TNF-α or IL-1β, are not only NFkB activators, but also its downstream transcriptional targets [23,26]. ADA treatment increased the expression of *IL1B* and *TNFA* genes by 73.3 ± 20.8- and 5.9 ± 0.6-fold, respectively ($p < 0.0005$; Fig. 4A). Notably, quantitative RT-PCR results showed very low basal expression of these cytokines in control cells. Likewise, the IL-1β cytokine is virtually undetectable by Western blot in control cells (Fig. 4B), although its expression is significantly augmented by ADA (50.4 ± 4.8-fold; $p < 0.0005$). We next examined whether inhibiting NFkB pathways modulates ADA-induced cytokine expression (Fig. 4C). Unexpectedly, the ADA-induced up-regulation of *IL1B* expression was 63.1 ± 3.2% lower when the cells were infected with AdCtrl (compared to uninfected cells exposed to ADA), but still significantly increased compared with cells not exposed to the SAH hydrolase inhibitor (12.8 ± 1.1-fold; $p < 0.0005$). IkBDN reduced the ADA-induced expression of *IL1B* by 63.4 ± 2.4% compared to the ADA-treated AdCtrl ($p < 0.0005$); however, IkBDN failed to eliminate completely ADA-induced *IL1B* up-regulation as *IL1B* expression remained 7.7 ± 0.5-fold higher in IKBDN expressing cells with ADA compared to untreated IkBDN expressing cells ($p < 0.005$). ADA-treated cells infected with the AdCtrl had substantially greater expression of *TNFA* when compared with uninfected cells exposed to ADA ($p < 0.0005$; Fig. 4C); nonetheless, *TNFA* up-regulation by ADA was completely abolished by IkBDN expression ($p < 0.0005$).

3.5. Excess SAH disturbs EZH2 and EZH2-related proteins

Previous studies have shown that SAHH inhibitors can suppress the activity of the S-adenosylmethionine-dependent methyltransferase EZH2 [27]. The balance between the activity of EZH2 and the demethylase JMJD3 modulates epigenetic regulation through H3K27me3. EZH2 is known to suppress the expression of the senescence markers, cyclin-dependent kinase inhibitor 1A (CDKN1A/p21) and 2A (CDKN2A/p16) [28].

To determine whether EZH2 was altered by SAHH inhibition in HCAEC, we investigated the effects of ADA on the expression of *EZH2*; the EZH2-regulated genes, *CDKN1A* and *CDKN2A*; and *KDM6B*, which encodes the demethylase JMJD3 (Fig. 5A). ADA treatment resulted in a 58.0 ± 11.7 and 68.4 ± 7.7% reduction of *EZH2* and *KDM6B* mRNA levels, respectively ($p < 0.005$). *CDKN1A* gene expression was 2.1 ± 0.3-fold

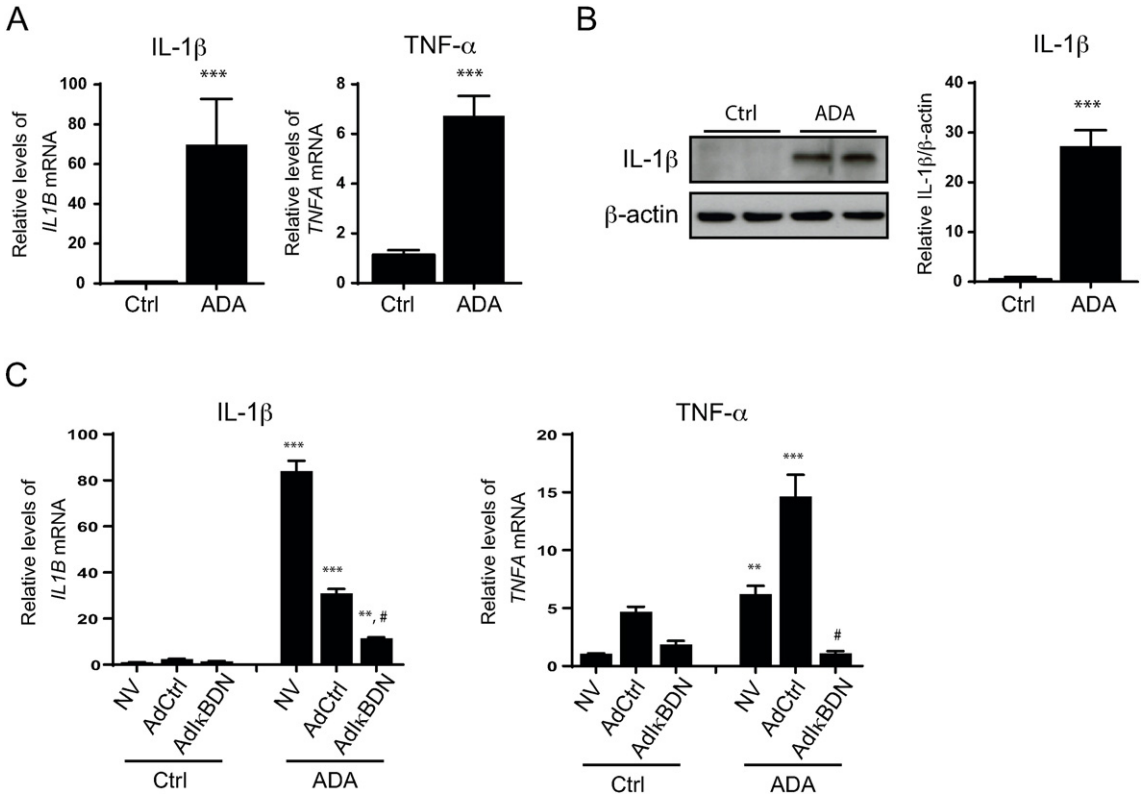

Fig. 4. Expression of proinflammatory cytokines under SAH accumulation. A, *IL1B* and *TNFA* mRNA were measured by quantitative RT-PCR for control and ADA-treated cells (n = 4). ***p < 0.0005, versus control. B, Western blot analysis of IL-1β protein expression induced by ADA treatment. A representative blot is shown. Mean densitometry results are presented. Statistical significance was measured as in A. C, Cytokine mRNA expression was determined for control and ADA treated cells infected with the adenovirus IkBDN (AdIkBDN), a control adenovirus (AdCtrl), or no virus (NV) by quantitative RT-PCR (n = 3–4). A multiple comparison ANOVA statistical analysis was performed, and the significance of the differences between the means is indicated. ***p < 0.0005, **p < 0.005 versus corresponding condition without ADA; #p < 0.005, compared to ADA treated no virus or ADA treated AdCtrl.

higher after ADA treatment ($p < 0.005$), whereas *CDKN2A* expression was not significantly changed. EZH2 protein levels decreased by 59.8 ± 0.1% with ADA treatment ($p < 0.005$; Fig. 5B). SAH accumulation also decreased H3K27me3 content by 25.5 ± 0.2% ($p < 0.05$; Fig. 5C), consistent with a decrease in cellular EZH2 activity. Fig. 5D suggests that SAH-mediated changes in EZH2 expression and activity are independent of NFkB activation, as the presence of IkBDN had no effect on ADA-induced suppression of EZH2 nor did it alter the ADA-induced increase of CDKN1A.

3.6. EZH2 knockdown mimics SAH-mediated effects on cell activation

To determine whether ADA-induced EZH2 suppression could contribute to the pro-inflammatory activation of endothelial cells, we knocked down EZH2 using a targeted siRNA (siEZH2) and analyzed the expression of adhesion molecules and CDKN1A, as well as IL-1β, another known target of EZH2-associated epigenetic regulation [16]. EZH2 knockdown resulted in a 94.1 ± 0.9 and 73.3 ± 8.9% reduction of EZH2 mRNA and protein levels, respectively ($p < 0.005$ vs siCtrl; Fig. 6). Suppression of EZH2 expression increased CDKN1A mRNA and protein levels when compared to siCtrl treated cells by 2.3 ± 0.4- and 1.3 ± 0.1-fold, respectively ($p < 0.005$). [The up-regulation of CDKN1A gene expression was also significant when comparing the siEZH2 and nontransfected cells, but the protein levels were not significantly different between these groups.] A significant increase of 4.8 ± 1.4- and 2.6 ± 0.5-fold was also observed for *ICAM1* and *VCAM1* expression following EZH2 knockdown compared to siCtrl conditions ($p < 0.05$). The role of EZH2 on the expression of adhesion molecules was further confirmed by Western blot, where EZH2 knockdown resulted in a 1.5 ± 0.1-fold increase of ICAM-1 expression ($p < 0.0005$, Fig. 6B). EZH2 knockdown also resulted in a 7.3 ± 2.1-fold increase of IL-1β mRNA levels compared to siCtrl conditions ($p < 0.005$).

To determine whether EZH2 inhibition could promote NFkB activation, we monitored IkBα degradation after EZH2 knockdown. Cells transfected with siEZH2 showed 23.0 ± 7.6% less IkBα than those transfected with the siCtrl ($p < 0.05$). Furthermore, EZH2 knockdown increased *NFKB2* gene expression 2.3 ± 0.4-fold ($p < 0.005$), supporting a possible role for EZH2 in modulating NFkB pathways in endothelial cells.

4. Discussion

The role of homocysteine as a risk factor for cardiovascular disease (CVD) has been widely debated. SAH, as a functionally important metabolite of homocysteine metabolism, has been suggested as a potentially more accurate indicator and determinant of CVD risk [29–31]. Excess SAH is a potent inhibitor of most SAM-dependent methyltransferases, and the SAM/SAH ratio has been used as a marker for the methylation potential. Perna et al. [32] hypothesized that the lower SAM/SAH ratio found in erythrocytes of chronic renal failure patients contributed to the reduction of erythrocyte membrane protein carboxyl methylation due to an inhibition of transmethylation reactions. Many subsequent studies in cultured cells as well as in in vivo systems support the concept that a decreased SAM/SAH ratio inhibits some methyltransferases resulting in hypomethylation of macromolecules [1,3,4,6,33–36]. In HUVEC, ADA-induced suppression of SAH hydrolase leads to an approximate 6-fold decrease in the SAM/SAH ratio. In HCAEC, we found that ADA induced an approximate 16-fold decrease in this ratio. In hyperhomocysteinemia caused by cystathionine beta-synthase deficiency in mice [36], the SAM/SAH ratio was decreased by 2.4- to 25-fold in various tissues compared to control mice, whereas vitamin B_6-deficiency in rodents induced hyperhomocysteinemia with an approximate 2- to 7-fold decrease in plasma and liver SAM/SAH ratio in various studies [37,38]. Similarly, the SAM/SAH ratio was

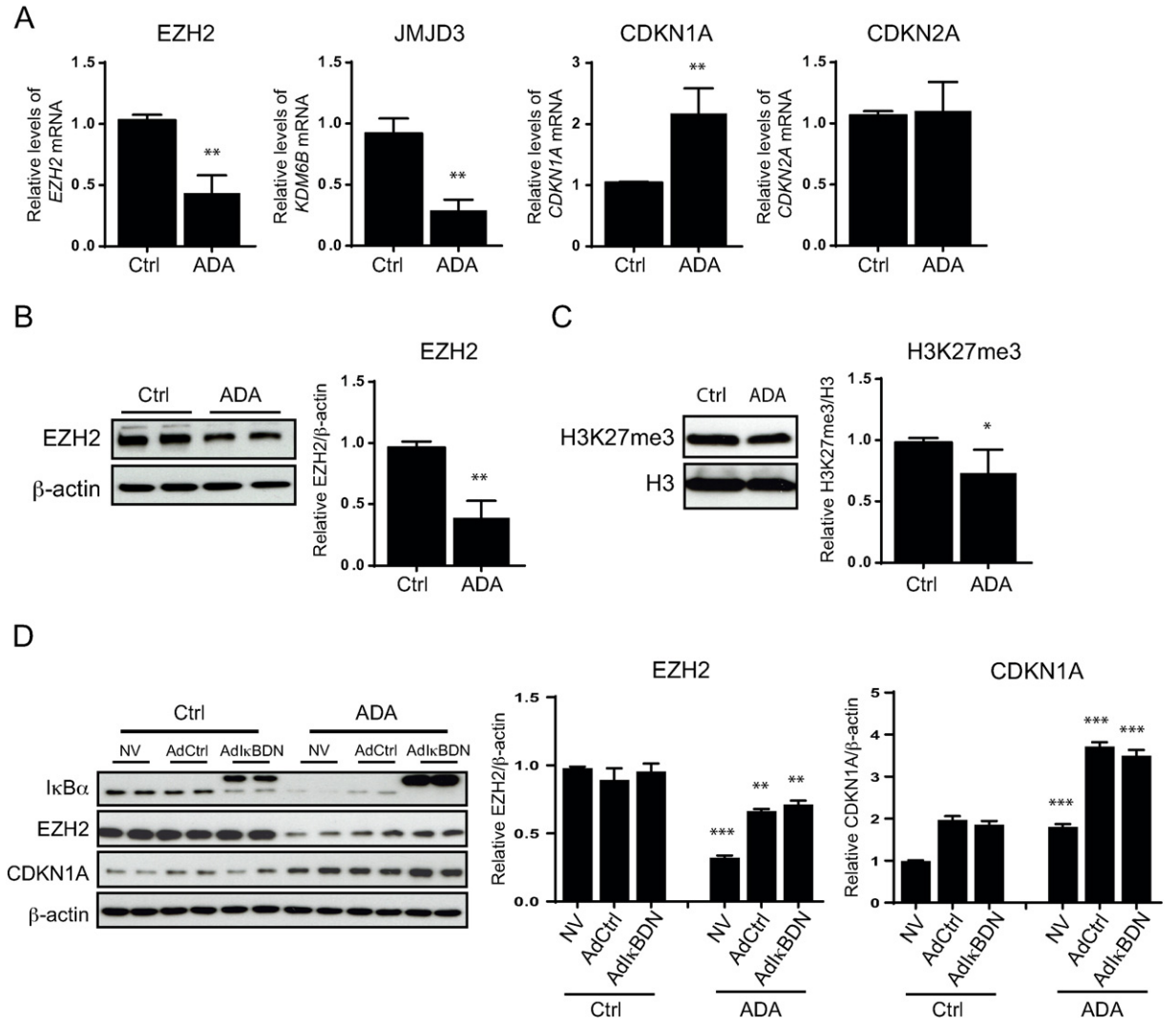

Fig. 5. Effects of excess SAH on EZH2 and EZH2-related proteins. A, *EZH2*, *KDM6B* (encoding JMJD3), *CDKN1A*, *and CDKN2A* mRNA levels were studied by quantitative RT-PCR following ADA treatment (n = 3). **p < 0.005, versus control. B, Total protein extracts from control and ADA treated cells were used for Western blot detection of EZH2. A representative blot is shown on the left and the summary of densitometry analysis on the right (n = 3). Statistical analysis was performed as in A. C, Western blot analysis of histone H3K27 tri-methylation (H3K27me3) after ADA treatment. Data are analyzed as in A. *p < 0.05, versus control. D, EZH2 and CDKN1A protein expression was evaluated, by Western blot, in noninfected cells (NV) or those infected with the adenovirus IkBDN or adenovirus control (AdCtrl) in the presence or absence of ADA treatment. Representative blots are presented along with densitometry analysis (n = 3–4). An ANOVA multiple comparisons test was used to analyze the statistically significant differences between means. **p < 0.005, ***p < 0.0005, versus the corresponding condition without ADA treatment.

decreased 4–8-fold in erythrocytes from human subjects with chronic renal failure, a condition that causes hyperhomocysteinemia, as compared to the ratio in normal control erythrocytes [32]. Thus, the decrease in SAM/SAH induced in cell culture by pharmacological means is within the range reported for in vivo hyperhomocysteinemia and consistent with changes capable of causing hypomethylation. Interestingly, atherosclerosis was augmented by in vivo administration of ADA or an SAH hydrolase short hairpin RNA in ApoE$^{-/-}$ mice under conditions that modestly increased plasma SAH and decreased (by 2-fold) SAM/SAH [6], suggesting that SAH contributes to atherogenesis.

Our work has focused on targets that are impaired by excess SAH that may contribute to vascular disease development. We have shown that SAH hydrolase inhibition disturbs nitric oxide production and inhibits antioxidant systems in HUVECs [1,8]. Here, we used primary endothelial cells derived from coronary arteries (HCAECs) to examine the mechanisms by which SAH promotes inflammatory activation. The adhesion of leukocytes to endothelial cells, which occurs during inflammatory diseases such as atherosclerosis, is complex and involves multiple interactions among endothelial and leukocyte surface molecules. We monitored the expression of ICAM-1 and VCAM-1, as well as the expression of *SELE*, which encodes E-selectin, an adhesion molecule involved mainly in the early stages of the adhesion process, and *PECAM1*, which is required during the transmigration stage [39]. *SELE*, *ICAM1*, and *VCAM1* are all target genes for NFkB and were all significantly increased by ADA, suggesting that NFkB may be activated by excess SAH (Fig. 1). By contrast, *PECAM1* was significantly decreased by ADA treatment. Down-regulation of *PECAM1* expression upon cell activation has been shown previously in various cell models, including endothelial cells [40–43]. Notably, although its global expression may be decreased, its redistribution to the cell surface to favor leukocyte transmigration is likely [40–42,44]. In fact, in our previous work in HUVECs, we found evidence for increased cell surface expression of this adhesion molecule following cell activation by excess SAH [1].

We report a novel link between the hypomethylating agent SAH and NFkB activation. Using an NFkB luciferase reporter construct, we confirmed that ADA induced NFkB-dependent transcriptional activation. Our data support an activation of both the canonical and non-canonical NFkB pathways in endothelial cells. Thus, IkBα degradation and p65 nuclear migration were up-regulated and the expression and processing of p100 were enhanced by ADA. The crosstalk between

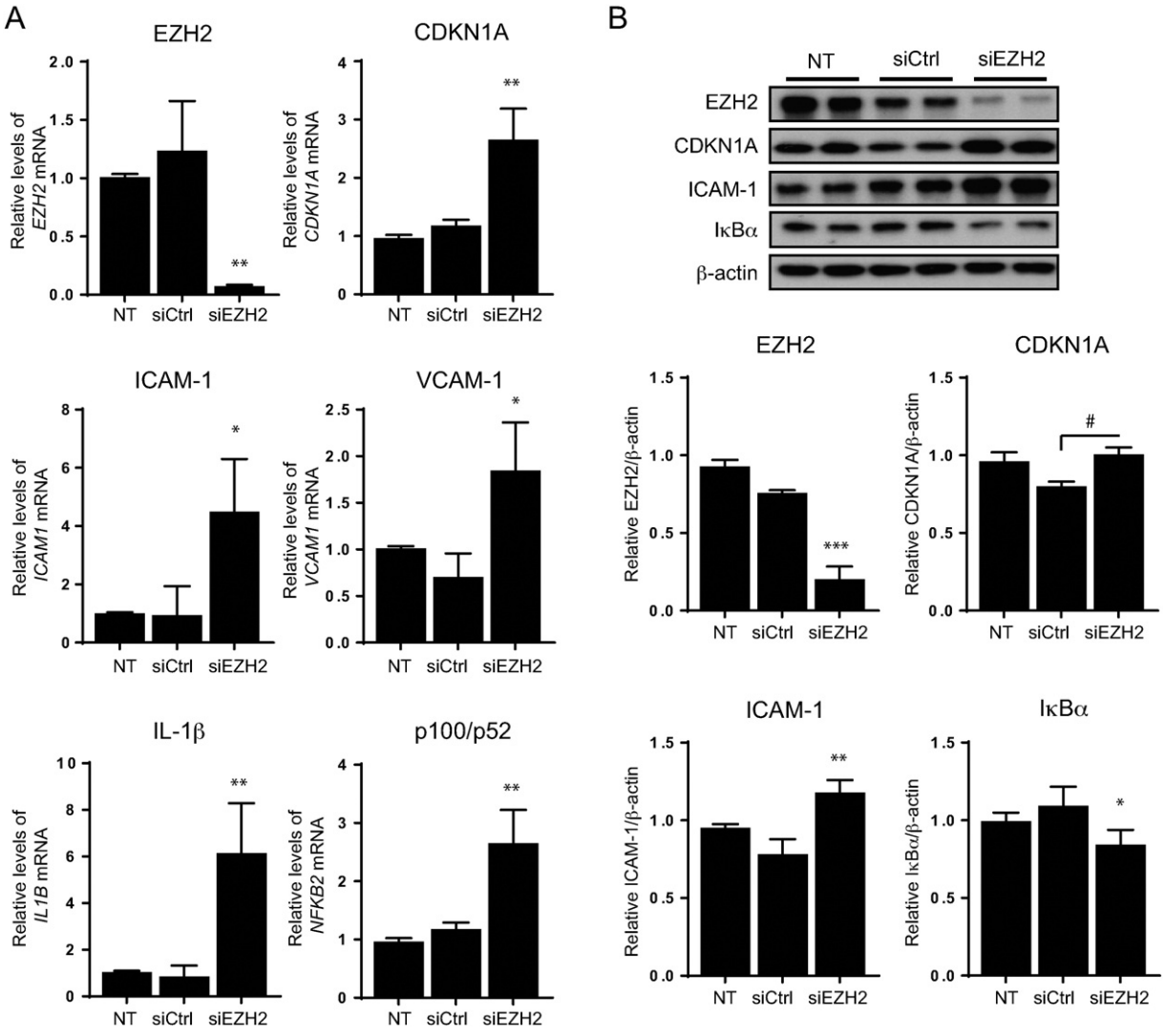

Fig. 6. Effects of EZH2 knockdown on NFkB and endothelial cell activation. A, Quantitative RT-PCR results are presented for non-transfected (NT) and transfected cells with either a scrambled siRNA (siCtrl) or an siRNA directed to EZH2 (siEZH2) (n = 3–4). B, Western blot analysis was performed after knockdown of EZH2. Representative blots (top) along with densitometry analysis (below) are shown (n = 3). Statistically significant differences between the means were determined by an ANOVA multiple comparisons test for panel A and B. *p < 0.05, **p < 0.005, ***p < 0.0005, versus the non-transfected and siCtrl conditions. #p < 0.0005 significant only against siCtrl.

canonical and non-canonical NFkB pathways is reported to exist at several different points in these activation cascades [45]. We found that the increased expression of the *NFKB2* gene (Fig. 3) was dependent on the activation of the canonical pathway following ADA treatment (Fig. 3C). The regulation of the *NFKB2* gene by the canonical NFkB pathway has been previously described; however, studies suggest that increased expression of p100 may have a positive or negative effect on the subsequent activation of the non-canonical pathway [45]. p100 is the precursor of p52 and required for non-canonical pathway activation, but its accumulation (without degradation to p52) can paradoxically lead to the suppression of RelB nuclear translocation [45,46]. In our cell system, excess SAH not only resulted in an NFkB-dependent *NFKB2* up-regulation, but also in increased processing of p100 to p52. The non-canonical NFkB pathway is largely involved in lymphoid organ development and adaptive immune responses. Its role in endothelial cell function is largely unknown [46,47]. Interestingly, the expression of CXCL2, which is a pro-inflammatory cytokine involved in lymphocyte transendothelial migration, was reported to be dependent on activation of the non-canonical NFkB pathway in endothelial cells [48,49]. Further investigation is necessary to clarify the role of the non-canonical NFkB pathway and *CXCL2* expression in SAH-induced endothelial cell activation.

NFkB pathways can be triggered by several factors, including pathogen exposure, inflammatory cytokines, radiation, and other stress signals [14,50]. Interestingly, pro-inflammatory cytokines, such as IL-1β and TNF-α, are not only NFkB targets, but also NFkB activators via their receptor-mediated actions. We found that SAH accumulation caused a significant increase in the expression of *IL1B* and *TNFA* (Fig. 4). IL-1β is synthesized as a precursor 33 kDa protein, which is cleaved by caspase-1, inducing the extracellular release of the processed 17 kDa form [51]. Only the precursor form was detectable by Western blot following ADA treatment (Fig. 4B). [The mature form of IL-1β was below the detection limit of the Western blot, possibly owing to its release from the cell and/or its low levels of production.] In order to understand whether increased cytokine production is a consequence of NFkB activation, we used the recombinant IkBDN. Our results show that IkBDN completely suppressed the ADA-induced increase of *TNFA*. IKBDN also significantly reduced, but did not eliminate, ADA-induced up-regulation of *IL1B*, as it remained elevated in comparison to untreated samples (Fig. 4C). These findings suggest that intracellular accumulation of SAH leads to cytokine production in response to NFkB activation, which may continue to augment and prolong cellular activation by promoting cytokine receptor-mediated activation of NFkB.

It is unclear why IkBDN failed to completely block the up-regulation of *IL1B* by ADA; however, the *IL1B* promoter may be additionally regulated by other pathways, independent of NFkB. Our previous studies showed that ADA induced oxidant stress in endothelial cells [1]. Specifically, hypomethylation led to the suppression of GPx1 and other selenocysteine containing enzymes, which play an important role in the maintenance of cell redox balance [1,52]. Other studies, including our own in microvascular endothelial cells, indicate that decreased GPx1 expression can enhance inflammatory signaling in response to cytokines and endotoxins by increasing oxidants [53,54]. In HCAECs, the use of antioxidants confirmed that oxidative stress also contributes to SAH-induced inflammatory activation; however, antioxidants were unable to eliminate ADA's effects on adhesion molecule up-regulation and failed to block ADA-induced IkB degradation in HCAECs (data not shown).

To understand better the effects of excess SAH on endothelial cell activation, we considered other pathways that might contribute to endothelial activation. Recently, decreased levels of H3K27me3 were positively correlated with the progression of atherosclerosis [55]. Here, we report that SAH accumulation can induce H3K27 hypomethylation (Fig. 5). The H3K27me3 repressive mark is maintained by EZH2 and can be removed by JMJD3. We investigated the endothelial changes in *EZH2* and *KDM6B* expression under SAH accumulation promoted by ADA. EZH2 is a possible target for SAH-directed inhibition, and our findings show that its gene expression is also decreased by excess SAH via an as-yet unknown mechanism. Furthermore, *KDM6B* gene expression was down-regulated with excess SAH, suggesting that a feedback mechanism may be triggered due to lack of substrate. Interestingly, it was recently reported in cancer cell lines that JMJD3 suppression can be mediated by miR-941, which is up-regulated with DNA hypomethylation [56]. Similarly, EZH2 expression has been shown to be suppressed by microRNAs that may normally be transcriptionally repressed by DNA methylation [57]. Thus, similar mechanisms could contribute to JMJD3 or EZH2 suppression by excess SAH.

EZH2 is known to mediate transcriptional repression of the cyclin-dependent kinase inhibitor *CDKN1A* and *CDKN2A* genes. CDKN1A and CDKN2A inhibit different cyclin-dependent kinases, contributing to a senescent phenotype by blocking cell cycle progression [28]. Expression of *CDKN1A*, but not *CDKN2A*, was significantly increased with SAH accumulation, most likely due to EZH2 inhibition, and suggesting that a senescent phenotype might be activated. Endothelial cell senescence has been associated with atherogenesis and could be another mechanism by which SAH contributes to vascular disease [58]. Previous studies have shown that under conditions that favor intracellular accumulation of SAH, homocysteine inhibits the growth of endothelial cells [34,35]. Specifically, the hypomethylation of $p21^{ras}$ was proposed to

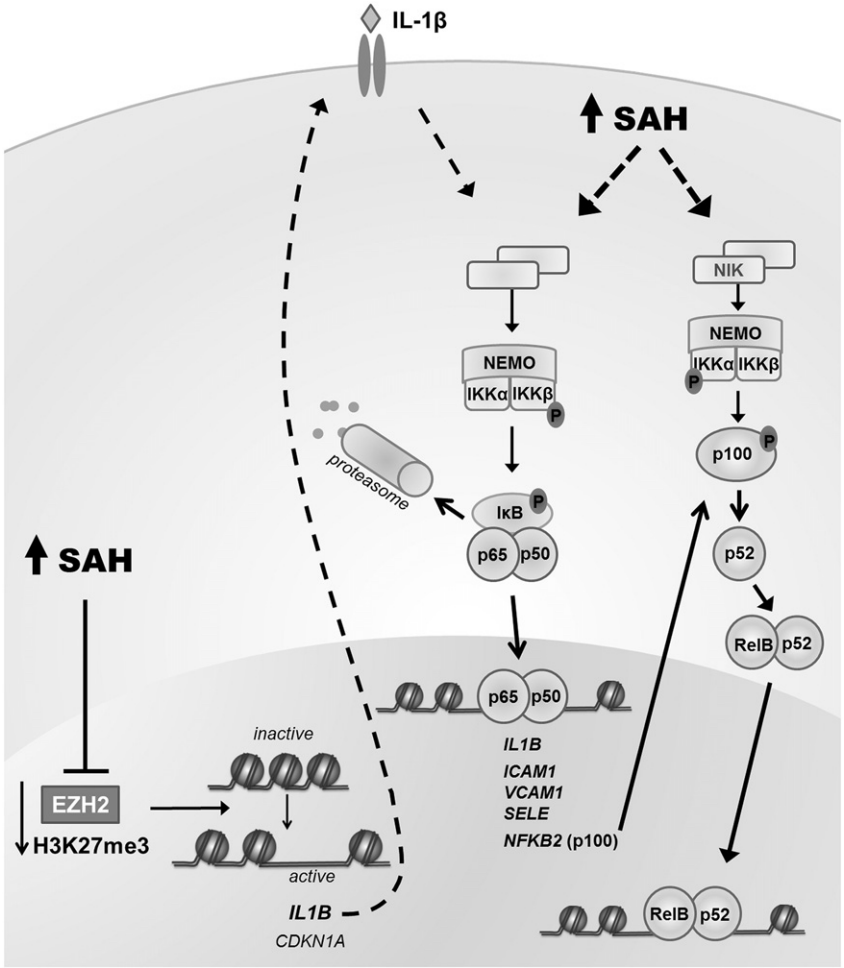

Fig. 7. Potential mechanism(s) by which SAH causes endothelial activation. SAH can inhibit EZH2 activity, decreasing the repressive histone mark H3K27me3. H3K27me3 suppresses the expression of a number of genes, including *CDKN1A* and *IL1B*. By stimulating its receptor, IL-1β can contribute to NFkB activation. Exposure to excess SAH activates both the canonical and non-canonical NFkB pathways. The canonical pathway involves IκB kinase complex (IKK) activation to induce IkB phosphorylation, triggering its ubiquitination-mediated degradation by the proteasome. Following IkB degradation, NFkB complexes (p65/p50) are free to migrate to the nucleus, activating transcription of its target genes. SAH induces NFkB-mediated transcription of cytokines (such as IL-1β, which can sustain further NFkB activation), adhesion molecules, and *NFkB2*. The non-canonical pathway relies on the activation of NFkB-interacting kinase (NIK) and IKKα which mediates the phosphorylation of the *NFkB2* gene product, p100, leading to its processing to p52, and subsequent migration of RelB/p52 to the nucleus. SAH augments the accumulation of p52, which may contribute to endothelial cell activation.

decrease endothelial cell growth as it alters the membrane localization of this protein [34]. Similarly, hypomethylation of the cyclin A gene correlated with its reduced transcription in endothelial cells, most likely due to the effects of a transcriptional inhibitor that can bind to the unmethylated DNA [35]; the resulting deficiency of cyclin A arrested cell cycle transition at the G1/S phase. We also observed decreased cell growth in cells treated with ADA (data not shown); however, additional studies are necessary to determine whether loss of EZH2 methyltransferase activity and increased expression of CDKN1A contribute to SAH-mediated growth suppression in endothelial cells.

Little is known about the interaction of EZH2 with the NFkB pathway, especially in endothelial cells. In breast cancer cells, the EZH2 protein caused an activation or repression of NFkB pathways depending on the estrogen receptor (ER) status of the cancer cells [59]. In ER-negative cancer cells, EZH2 physically interacted with NFkB heterodimers to promote the expression of a subset of NFkB target genes; whereas in ER-positive cells, ER recruited EZH2-containing complexes to NFkB target genes to epigenetically silence them via histone methylation. A different interaction was found between NFkB and EZH2 in endothelial cells infected with Kaposi sarcoma-associated herpesvirus in which latent viral genes were found to activate NFkB, leading to increased expression of EZH2 [60]. In primary endothelial cells, we found a different association between EZH2 and NFkB that was caused by a loss of functional EZH2. In fact, NFkB had no effect on EZH2 expression in HCAECs; rather, the loss of EZH2 promoted NFkB activation, with a concomitant increase of NFkB2 mRNA levels.

In support of a role for EZH2 suppression in ADA-induced activation of NFkB, knockdown of EZH2 (Fig. 6) recapitulated the effects of ADA, activating NFkB and increasing the expression of adhesion molecules and the pro-inflammatory cytokine *IL1B*. Although the pro-inflammatory effects of EZH2 knockdown are less robust than those induced by SAH hydrolase inhibition, the knockdown caused many of the same inflammatory responses. It is likely that the magnitude of these responses is lower with EZH2 knockdown as additional pathways (such as oxidative stress) that also contribute to endothelial cell dysfunction may be activated by SAH-accumulation. Nonetheless, our results support a role for EZH2 suppression in the effects of excess SAH, and suggest that EZH2 suppression may contribute to NFKB activation in endothelial cells.

In conclusion, our studies implicate homocysteine's precursor, SAH, in the activation of the canonical and non-canonical NFkB pathways. Furthermore, excess SAH suppresses EZH2, decreasing the global levels of the repressive H3K27me3 mark. Based on these results, we believe that EZH2 suppression promotes the expression of inflammatory cytokines, such as IL-1β, due to a decrease of the epigenetic mark H3K27me3 at the *IL1B* promoter [16,26]. Up-regulation of IL-1β may promote the continued stimulation of the NFkB pathway via activation of the IL-1β receptor. Thus, we suggest that SAH-induced EZH2 suppression can contribute to pro-inflammatory changes favoring atherogenesis. Our results reveal an important link between NFkB and PRC2 epigenetic regulation, which may be relevant to vascular disease (Fig. 7).

Transparency document

The Transparency document associated with this article can be found in the online version.

Funding and acknowledgments

This work was supported by NIH grants HL061795, HL048743, HL108630 and HL119145 (to JL) and by the Portuguese Fundação para a Ciência e a Tecnologia grant SFRH/BD/73021/2010 (to MB). The authors also wish to thank Ms. Johana Kugele for support in the assays of SAM and SAH and Ms. Stephanie Tribuna for expert technical assistance in preparing this manuscript.

References

[1] M. Barroso, C. Florindo, H. Kalwa, Z. Silva, A.A. Turanov, B.A. Carlson, et al., Inhibition of cellular methyltransferases promotes endothelial cell activation by suppressing glutathione peroxidase 1 protein expression, J. Biol. Chem. 289 (2014) 15350–15362, http://dx.doi.org/10.1074/jbc.M114.549782.
[2] M.A. Caudill, J.C. Wang, S. Melnyk, I.P. Pogribny, S. Jernigan, M.D. Collins, et al., Intracellular S-adenosylhomocysteine concentrations predict global DNA hypomethylation in tissues of methyl-deficient cystathionine beta-synthase heterozygous mice, J. Nutr. 131 (2001) 2811–8.
[3] R. Esse, C. Florindo, A. Imbard, M.S. Rocha, A.S. de Vriese, Y.M. Smulders, et al., Global protein and histone arginine methylation are affected in a tissue-specific manner in a rat model of diet-induced hyperhomocysteinemia, Biochim. Biophys. Acta 1832 (2013) 1708–1714, http://dx.doi.org/10.1016/j.bbadis.2013.05.013.
[4] R. Castro, I. Rivera, E.A. Struys, E.E.W. Jansen, P. Ravasco, M.E. Camilo, et al., Increased homocysteine and S-adenosylhomocysteine concentrations and DNA hypomethylation in vascular disease, Clin. Chem. 49 (2003) 1292–1296.
[5] R. Clarke, L. Daly, K. Robinson, E. Naughten, S. Cahalane, B. Fowler, et al., Hyperhomocysteinemia: an independent risk factor for vascular disease, N. Engl. J. Med. 324 (1991) 1149–1155, http://dx.doi.org/10.1056/NEJM199104253241701.
[6] Y. Xiao, W. Huang, J. Zhang, C. Peng, M. Xia, W. Ling, Increased plasma S-adenosylhomocysteine-accelerated atherosclerosis is associated with epigenetic regulation of endoplasmic reticulum stress in apoE −/− mice, Arterioscler. Thromb. Vasc. Biol. 35 (2015) 60–70, http://dx.doi.org/10.1161/ATVBAHA.114.303817.
[7] A.M. Zawada, K.S. Rogacev, B. Hummel, J.T. Berg, A. Friedrich, H.J. Roth, et al., S-adenosylhomocysteine is associated with subclinical atherosclerosis and renal function in a cardiovascular low-risk population, Atherosclerosis 234 (2014) 17–22, http://dx.doi.org/10.1016/j.atherosclerosis.2014.02.002.
[8] M. Barroso, M.S. Rocha, R. Esse, I. Gonçalves, A.Q. Gomes, T. Teerlink, et al., Cellular hypomethylation is associated with impaired nitric oxide production by cultured human endothelial cells, Amino Acids 42 (2012) 1903–1911, http://dx.doi.org/10.1007/s00726-011-0916-0.
[9] R. Gareus, E. Kotsaki, S. Xanthoulea, I. van der Made, M.J.J. Gijbels, R. Kardakaris, et al., Endothelial cell-specific NF-kappaB inhibition protects mice from atherosclerosis, Cell Metab. 8 (2008) 372–383, http://dx.doi.org/10.1016/j.cmet.2008.08.016.
[10] D.E. Handy, E. Lubos, Y. Yang, J.D. Galbraith, N. Kelly, Y.-Y. Zhang, et al., Glutathione peroxidase-1 regulates mitochondrial function to modulate redox-dependent cellular responses, J. Biol. Chem. 284 (2009) 11913–11921, http://dx.doi.org/10.1074/jbc.M900392200.
[11] B. Pamukcu, G.Y.H. Lip, E. Shantsila, The nuclear factor-kappa B pathway in atherosclerosis: a potential therapeutic target for atherothrombotic vascular disease, Thromb. Res. 128 (2011) 117–123, http://dx.doi.org/10.1016/j.thromres.2011.03.025.
[12] R. Madonna, R. De Caterina, Relevance of new drug discovery to reduce NF-κB activation in cardiovascular disease, Vasc. Pharmacol. 57 (2012) 41–47, http://dx.doi.org/10.1016/j.vph.2012.02.005.
[13] G. Gloire, S. Legrand-Poels, J. Piette, NF-kappaB activation by reactive oxygen species: fifteen years later, Biochem. Pharmacol. 72 (2006) 1493–1505, http://dx.doi.org/10.1016/j.bcp.2006.04.011.
[14] M. Hinz, C. Scheidereit, The IκB kinase complex in NF-κB regulation and beyond, EMBO Rep. 15 (2014) 46–61, http://dx.doi.org/10.1002/embr.201337983.
[15] G. Deb, A.K. Singh, S. Gupta, EZH2: not EZHY (easy) to deal, Mol. Cancer Res. 12 (2014) 639–653, http://dx.doi.org/10.1158/1541-7786.MCR-13-0546.
[16] H. Dreger, A. Ludwig, A. Weller, V. Stangl, G. Baumann, S. Meiners, et al., Epigenetic regulation of cell adhesion and communication by enhancer of zeste homolog 2 in human endothelial cells, Hypertension 60 (2012) 1176–1183, http://dx.doi.org/10.1161/HYPERTENSIONAHA.112.191098.
[17] M.R. Hübner, D.L. Spector, Role of H3K27 demethylases Jmjd3 and UTX in transcriptional regulation, Cold Spring Harb. Symp. Quant. Biol. 75 (2010) 43–49, http://dx.doi.org/10.1101/sqb.2010.75.020.
[18] K. Agger, P.A.C. Cloos, J. Christensen, D. Pasini, S. Rose, J. Rappsilber, et al., UTX and JMJD3 are histone H3K27 demethylases involved in HOX gene regulation and development, Nature 449 (2007) 731–734, http://dx.doi.org/10.1038/nature06145.
[19] K. Williams, J. Christensen, J. Rappsilber, A.L. Nielsen, J.V. Johansen, K. Helin, The histone lysine demethylase JMJD3/KDM6B is recruited to p53 bound promoters and enhancer elements in a p53 dependent manner, PLoS ONE 9 (2014), e96545. http://dx.doi.org/10.1371/journal.pone.0096545.
[20] H. Gellekink, D. van Oppenraaij-Emmerzaal, A. van Rooij, E.A. Struys, M. den Heijer, H.J. Blom, Stable-isotope dilution liquid chromatography–electrospray injection tandem mass spectrometry method for fast, selective measurement of S-adenosylmethionine and S-adenosylhomocysteine in plasma, Clin. Chem. 51 (2005) 1487–1492, http://dx.doi.org/10.1373/clinchem.2004.046995.
[21] M.T. Harte, J.J. Gorski, K.I. Savage, J.W. Purcell, E.M. Barros, P.M. Burn, et al., NF-κB is a critical mediator of BRCA1-induced chemoresistance, Oncogene 33 (2014) 713–723, http://dx.doi.org/10.1038/onc.2013.10.
[22] F. Mackay, Tumor necrosis factor alpha (TNF-alpha)-induced cell adhesion to human endothelial cells is under dominant control of one TNF receptor type, TNF-R55, J. Exp. Med. 177 (1993) 1277–1286, http://dx.doi.org/10.1084/jem.177.5.1277.
[23] B. Hoesel, J.A. Schmid, The complexity of NF-κB signaling in inflammation and cancer, Mol. Cancer 12 (2013) 86, http://dx.doi.org/10.1186/1476-4598-12-86.
[24] A. Leychenko, E. Konorev, M. Jijiwa, M.L. Matter, Stretch-induced hypertrophy activates NFkB-mediated VEGF secretion in adult cardiomyocytes, PLoS ONE 6 (2011), e29055, http://dx.doi.org/10.1371/journal.pone.0029055.
[25] S. Choudhary, M. Kalita, L. Fang, K.V. Patel, B. Tian, Y. Zhao, et al., Inducible tumor necrosis factor (TNF) receptor-associated factor-1 expression couples the canonical to the non-canonical NF-κB pathway in TNF stimulation, J. Biol. Chem. 288 (2013) 14612–14623, http://dx.doi.org/10.1074/jbc.M113.464081.

[26] M. Maleszewska, R.A.F. Gjaltema, G. Krenning, M.C. Harmsen, Enhancer of zeste homolog-2 (EZH2) methyltransferase regulates transgelin/smooth muscle-22α expression in endothelial cells in response to interleukin-1β and transforming growth factor-β2, Cell. Signal. 27 (2015) 1589–1596, http://dx.doi.org/10.1016/j.cellsig.2015.04.008.
[27] P.-P. Kung, B. Huang, L. Zehnder, J. Tatlock, P. Bingham, C. Krivacic, et al., SAH derived potent and selective EZH2 inhibitors, Bioorg. Med. Chem. Lett. 25 (2015) 1532–1537, http://dx.doi.org/10.1016/j.bmcl.2015.02.017.
[28] J. Bai, J. Chen, M. Ma, M. Cai, F. Xu, G. Wang, et al., Inhibiting enhancer of zeste homolog 2 promotes cellular senescence in gastric cancer cells SGC-7901 by activation of p21 and p16, DNA Cell Biol. 33 (2014) 337–344, http://dx.doi.org/10.1089/dna.2014.2340.
[29] C. Wagner, M.J. Koury, S-adenosylhomocysteine: a better indicator of vascular disease than homocysteine? Am. J. Clin. Nutr. 86 (2007) 1581–1585.
[30] Y. Xiao, Y. Zhang, M. Wang, X. Li, D. Su, J. Qiu, et al., Plasma S-adenosylhomocysteine is associated with the risk of cardiovascular events in patients undergoing coronary angiography: a cohort study, Am. J. Clin. Nutr. 98 (2013) 1162–1169, http://dx.doi.org/10.3945/ajcn.113.058727.
[31] C. Liu, Q. Wang, H. Guo, M. Xia, Q. Yuan, Y. Hu, et al., Plasma S-adenosylhomocysteine is a better biomarker of atherosclerosis than homocysteine in apolipoprotein E-deficient mice fed high dietary methionine, J. Nutr 138 (2008) 311–315.
[32] A.F. Perna, D. Ingrosso, V. Zappia, P. Galletti, G. Capasso, N.G. De Santo, Enzymatic methyl esterification of erythrocyte membrane proteins is impaired in chronic renal failure. Evidence for high levels of the natural inhibitor S-adenosylhomocysteine, J. Clin. Invest. 91 (1993) 2497–2503, http://dx.doi.org/10.1172/JCI116485.
[33] D. Ingrosso, A. Cimmino, A.F. Perna, L. Masella, N.G. De Santo, M.L. De Bonis, et al., Folate treatment and unbalanced methylation and changes of allelic expression induced by hyperhomocysteinaemia in patients with uraemia, Lancet 361 (2003) 1693–1699, http://dx.doi.org/10.1016/S0140-6736(03)13372-7.
[34] H. Wang, M. Yoshizumi, K. Lai, J.C. Tsai, M.A. Perrella, E. Haber, et al., Inhibition of growth and p21ras methylation in vascular endothelial cells by homocysteine but not cysteine, J. Biol. Chem. 272 (1997) 25380–25385.
[35] M.D.S. Jamaluddin, I. Chen, F. Yang, X. Jiang, M. Jan, X. Liu, et al., Homocysteine inhibits endothelial cell growth via DNA hypomethylation of the cyclin A gene, Blood 110 (2007) 3648–3655, http://dx.doi.org/10.1182/blood-2007-06-096701.
[36] R. Esse, A. Imbard, C. Florindo, S. Gupta, E.P. Quinlivan, M. Davids, et al., Protein arginine hypomethylation in a mouse model of cystathionine β-synthase deficiency, FASEB J. 28 (2014) 2686–2695, http://dx.doi.org/10.1096/fj.13-246579.
[37] Y. Isa, H. Tsuge, T. Hayakawa, Effect of vitamin B6 deficiency on S-adenosylhomocysteine hydrolase activity as a target point for methionine metabolic regulation, J. Nutr. Sci. Vitaminol. 52 (2006) 302–306 (Tokyo).
[38] S. Taysi, M.S. Keles, K. Gumustekin, M. Akyuz, A. Boyuk, O. Cikman, et al., Plasma homocysteine and liver tissue S-adenosylmethionine, S-adenosylhomocysteine status in vitamin B6-deficient rats, Eur. Rev. Med. Pharmacol. Sci. 19 (2015) 154–160.
[39] W.A. Muller, Leukocyte–endothelial cell interactions in the inflammatory response, Lab. Investig. 82 (2002) 521–534, http://dx.doi.org/10.1038/labinvest.3780446.
[40] P.J. Newman, C.A. Hillery, R. Albrecht, L.V. Parise, M.C. Berndt, A.V. Mazurov, et al., Activation-dependent changes in human platelet PECAM-1: phosphorylation, cytoskeletal association, and surface membrane redistribution, J. Cell Biol. 119 (1992) 239–246.
[41] R.J. Stewart, T.S. Kashour, P.A. Marsden, Vascular endothelial platelet endothelial adhesion molecule-1 (PECAM-1) expression is decreased by TNF-alpha and IFN-gamma. Evidence for cytokine-induced destabilization of messenger ribonucleic acid transcripts in bovine endothelial cells, J. Immunol. 156 (1996) 1221–1228.
[42] Y. Sawa, Y. Sugimoto, T. Ueki, H. Ishikawa, A. Sato, T. Nagato, et al., Effects of TNF-alpha on leukocyte adhesion molecule expressions in cultured human lymphatic endothelium, J. Histochem. Cytochem. 55 (2007) 721–733, http://dx.doi.org/10.1369/jhc.6A7171.2007.
[43] J.L. Zehnder, K. Hirai, M. Shatsky, J.L. McGregor, L.J. Levitt, L.L. Leung, The cell adhesion molecule CD31 is phosphorylated after cell activation. Down-regulation of CD31 in activated T lymphocytes, J. Biol. Chem. 267 (1992) 5243–5249.
[44] L.H. Romer, N.V. McLean, H.C. Yan, M. Daise, J. Sun, H.M. DeLisser, IFN-gamma and TNF-alpha induce redistribution of PECAM-1 (CD31) on human endothelial cells, J. Immunol. 154 (1995) 6582–6592.
[45] S.-C. Sun, The noncanonical NF-κB pathway, Immunol. Rev. 246 (2012) 125–140, http://dx.doi.org/10.1111/j.1600-065X.2011.01088.x.
[46] S.-C. Sun, Non-canonical NF-κB signaling pathway, Cell Res. 21 (2011) 71–85, http://dx.doi.org/10.1038/cr.2010.177.
[47] A.R. Noort, K.P.M. van Zoest, E.M. Weijers, P. Koolwijk, C.X. Maracle, D.V. Novack, et al., NF-κB-inducing kinase is a key regulator of inflammation-induced and tumour-associated angiogenesis, J. Pathol. 234 (2014) 375–385, http://dx.doi.org/10.1002/path.4403.
[48] L.A. Madge, M.S. Kluger, J.S. Orange, M.J. May, Lymphotoxin-alpha 1 beta 2 and LIGHT induce classical and noncanonical NF-kappa B-dependent proinflammatory gene expression in vascular endothelial cells, J. Immunol. 180 (2008) 3467–3477.
[49] A.-R. Noort, K.P. van Zoest, P. Koolwijk, P.-P. Tak, S.W. Tas, NF-kappaB inducing kinase (NIK) is a key regulator of inflammation-induced angiogenesis, J. Transl. Med. 10 (2012) O1, http://dx.doi.org/10.1186/1479-5876-10-S3-O1.
[50] F. Liu, Y. Xia, A.S. Parker, I.M. Verma, IKK biology, Immunol. Rev. 246 (2012) 239–253, http://dx.doi.org/10.1111/j.1600-065X.2012.01107.x.
[51] U. Schönbeck, F. Mach, J.Y. Bonnefoy, H. Loppnow, H.D. Flad, P. Libby, Ligation of CD40 activates interleukin 1beta-converting enzyme (caspase-1) activity in vascular smooth muscle and endothelial cells and promotes elaboration of active interleukin 1beta, J. Biol. Chem. 272 (1997) 19569–19574.
[52] L.V. Papp, J. Lu, A. Holmgren, K.K. Khanna, From selenium to selenoproteins: synthesis, identity, and their role in human health, Antioxid. Redox Signal. 9 (2007) 775–806, http://dx.doi.org/10.1089/ars.2007.1528.
[53] E. Lubos, C.E. Mahoney, J.A. Leopold, Y.-Y. Zhang, J. Loscalzo, D.E. Handy, Glutathione peroxidase-1 modulates lipopolysaccharide-induced adhesion molecule expression in endothelial cells by altering CD14 expression, FASEB J. 24 (2010) 2525–2532, http://dx.doi.org/10.1096/fj.09-147421.
[54] E. Lubos, N.J. Kelly, S.R. Oldebeken, J.A. Leopold, Y.-Y. Zhang, J. Loscalzo, et al., Glutathione peroxidase-1 deficiency augments proinflammatory cytokine-induced redox signaling and human endothelial cell activation, J. Biol. Chem. 286 (2011) 35407–35417, http://dx.doi.org/10.1074/jbc.M110.205708.
[55] R.J. Wierda, I.M. Rietveld, M.C.J.A. van Eggermond, J.A.M. Belien, E.W. van Zwet, J.H.N. Lindeman, et al., Global histone H3 lysine 27 triple methylation levels are reduced in vessels with advanced atherosclerotic plaques, Life Sci. (2014). http://dx.doi.org/10.1016/j.lfs.2014.10.010.
[56] P.-P. Zhang, X.-L. Wang, W. Zhao, B. Qi, Q. Yang, H.-Y. Wan, et al., DNA methylation-mediated repression of miR-941 enhances lysine (K)-specific demethylase 6B expression in hepatoma cells, J. Biol. Chem. 289 (2014) 24724–24735, http://dx.doi.org/10.1074/jbc.M114.567818.
[57] A.-Y. So, J.-W. Jung, S. Lee, H.-S. Kim, K.-S. Kang, DNA methyltransferase controls stem cell aging by regulating BMI1 and EZH2 through microRNAs, PLoS ONE 6 (2011), e19503http://dx.doi.org/10.1371/journal.pone.0019503.
[58] J.C. Wang, M. Bennett, Aging and atherosclerosis: mechanisms, functional consequences, and potential therapeutics for cellular senescence, Circ. Res. 111 (2012) 245–259, http://dx.doi.org/10.1161/CIRCRESAHA.111.261388.
[59] S.T. Lee, Z. Li, Z. Wu, M. Aau, P. Guan, R.K.M. Karuturi, et al., Context-specific regulation of NF-κB target gene expression by EZH2 in breast cancers, Mol. Cell 43 (2011) 798–810, http://dx.doi.org/10.1016/j.molcel.2011.08.011.
[60] M. He, W. Zhang, T. Bakken, M. Schutten, Z. Toth, J.U. Jung, et al., Cancer angiogenesis induced by Kaposi sarcoma-associated herpesvirus is mediated by EZH2, Cancer Res. 72 (2012) 3582–3592, http://dx.doi.org/10.1158/0008-5472.CAN-11-2876.